

ORIGINAL ARTICLE

Identification and clinical characteristics of a novel missense ADGRG1 variant in bilateral Frontoparietal Polymicrogyria: The electroclinical change from infancy to adulthood after Callosotomy in three siblings

Cheng-Yen Kuo¹  | Meng-Han Tsai^{2,3}  | Hsi-Hsien Lin⁴ | Yu-Chi Wang⁵ |
 Abhishek Kumar Singh⁶ | Chang-Chih Chen⁷ | Jainn-Jim Lin^{1,2,8} | Po-Cheng Hung^{1,2} |
 Kuang-Lin Lin^{1,2}

¹Division of Pediatric Neurology, Chang Gung Children's Hospital and Chang Gung Memorial Hospital, Taoyuan, Taiwan

²School of Medicine, College of Medicine, Chang Gung University, Taoyuan, Taiwan

³Department of Neurology, Kaohsiung Chang Gung Memorial Hospital, Kaohsiung, Taiwan

⁴Department of Microbiology and Immunology, College of Medicine, Chang Gung University, Taoyuan, Taiwan

⁵Department of Neurosurgery, Chang Gung Memorial Hospital at Linkou, Chang Gung University, Taoyuan, Taiwan

⁶Department of Biological Sciences, Indian Institute of Science Education and Research, Mohali, India

⁷Department of Medical Imaging and Intervention, Chang Gung Memorial Hospital, Linkou, Chang Gung University, Taoyuan, Taiwan

⁸Division of Pediatric Critical Care and Pediatric Neurocritical Care Center, Chang Gung Children's Hospital and Chang Gung Memorial Hospital, Taoyuan, Taiwan

Correspondence

Kuang-Lin Lin, Division of Pediatric Neurology, Chang Gung Children's Hospital, 5 Fu-Shin Street, Kwei-Shan, Taoyuan, 333, Taiwan.
 Email: linckgh@cgmh.org.tw

Abstract

Objective: Bilateral frontoparietal polymicrogyria (BFPP) is a rare genetic-related migration disorder. It has been attributed to loss-of-function of the ADGRG1 gene, which encodes an adhesion G protein-coupled receptor, ADGRG1/GPR56. We report the EEG findings of BFPP in three Asian patients, and confirmed that change in protein function was caused by the novel missense variant (p.Leu290Pro).

Methods: We reviewed the medical records of three siblings with BFPP including one elder girl and two identical twin boys from birth to adulthood. The clinical symptoms, electroencephalography (EEG), brain MRI, whole-exome sequencing, treatment including medications, neuromodulation, and epilepsy surgery, and clinical outcomes were reviewed. The protein structure of a novel missense variant (p.Leu290Pro) was predicted by in silico analyses, and molecular analysis was performed via typical flow cytometry and Western blotting.

Results: The elder girl (Patient 1) was 22 years old and the twin boys (Patients 2 and 3) were 20 years old at the time of publication. All of them presented with typical clinical symptoms/signs and MRI findings of BFPP. Whole-exome sequencing followed by Sanger confirmation showed that all three patients had compound heterozygous variants in the ADGRG1 gene. The missense variant (p.Leu290Pro) was confirmed to be related to a reduction in cell surface GPR56 expression. High-amplitude rhythmic activity was noted in sleep EEG during infancy, which may have been due to excessive sleep spindle, and the rhythm disappeared when they were of pre-school age. Partial callosotomy provided short-term benefits in seizure control in Patients 1 and 2, and combined vagus nerve stimulation and partial callosotomy provided longer benefits in Patient 3.

This is an open access article under the terms of the [Creative Commons Attribution-NonCommercial-NoDerivs](https://creativecommons.org/licenses/by-nc-nd/4.0/) License, which permits use and distribution in any medium, provided the original work is properly cited, the use is non-commercial and no modifications or adaptations are made.

© 2022 The Authors. *Epilepsia Open* published by Wiley Periodicals LLC on behalf of International League Against Epilepsy.

Significance: Sleep EEG findings of high-amplitude rhythmic activity in our BFPP cases were only noted during infancy and childhood. We also confirmed that the missense variant (p.Leu290Pro) led to loss of function due to a reduction in cell surface GPR56 expression.

KEYWORDS

congenital CNS malformation, epilepsy, genetic, polymicrogyria

1 | INTRODUCTION

Polymicrogyria is a heterogeneous disease with diverse etiologies and clinical manifestations, ranging from nearly normal to severe disability. The etiologies, distribution of polymicrogyria, and association with other congenital central nervous system anomalies can all influence the clinical outcomes.¹ Bilateral frontoparietal polymicrogyria (BFPP) is an autosomal recessive genetic disease of cortical malformation caused by *ADGRG1/GPR56* gene deletion/mutation.² *ADGRG1/GPR56* belongs to the adhesion-class G-protein-coupled receptors (aGPCRs), which are characterized by an extended extracellular region (ECR).³ The N-terminal section of the aGPCR-ECR is normally composed of diverse cell-adhesive protein modules, whereas its C-terminal section consists of a signature GPCR autoproteolysis-inducing (GAIN) domain.⁴ As a result, most aGPCRs are processed by self-catalytic proteolysis at the consensus GPCR proteolysis site (GPS) of the GAIN domain to form a bipartite receptor complex comprised of an extracellular fragment and a seven-span transmembrane fragment.⁴ Several types of *ADGRG1/GPR56* genetic alterations including deletion, splicing, and missense mutations have been linked to BFPP.⁵ Interestingly, most BFPP-associated GPR56 missense point mutations have been identified at the ECR or extracellular loops. Moreover, all GPR56 missense variants are essentially null mutants, although they are functionally deficient due to diverse mechanisms including protein instability and stalled intracellular trafficking, inefficient GPS auto-proteolytic modification, and impaired receptor signaling.^{6,7} BFPP is thought to share common clinical symptoms and brain imaging characteristics with other glycosylation disorders, such as Walker-Warburg syndrome, muscle-eye-brain disease, and Fukuyama congenital muscular dystrophy.⁸ The clinical symptoms include developmental delay, impaired intelligence, disconjugate gaze, oral motor dyspraxia, pyramidal, cerebellum signs, and multiple types of epilepsy.⁹ The brain imaging characteristics of BFPP include white matter lesions and hypo/dysgenesis of the brainstem and cerebellum, which are not seen with other types of polymicrogyria.⁸ While the central nervous system structure anomalies described

Key Bullet Points

1. The first BFPP case series in Taiwan, and the first 20 years follow-up report in BFPP.
2. A special sleep EEG finding of high-amplitude rhythmic activity was found in the childhood period of BFPP patients before clinical seizure attack.
3. A new loss of function missense *ADGRG1* Variant (L290P) was proofed in three BFPP patients.
4. Corpus callosotomy promised excellent short-term benefit in epileptic drop attacks of BFPP patients and it combined with vagus nerve stimulation promised extra benefits.
5. Identical twins in BFPP patients could develop different seizure clinical course.

above remain mostly constant, the electroclinical symptoms usually evolve with age. However, detailed records of the evolution of the electroclinical symptoms in BFPP patients from birth to adulthood are limited. In addition, the effect of corpus callosotomy on seizure control in BFPP patients has not been investigated systematically.

Herein, we report the progression of changes in electroclinical patterns from infancy to adulthood and the effect of corpus callosotomy on seizure control in three siblings with BFPP in Taiwan. We identified and characterized a novel BFPP-causing *ADGRG1/GPR56* missense mutation, and showed that it was deficient in GPS proteolysis, intracellular trafficking, and cell surface expression.

2 | MATERIALS AND METHODS

2.1 | Clinical symptoms, signs, and medication records

We analyzed the electronic health records of three related patients with BFPP including one elder girl

(Patient 1) and two identical twin boys (Patients 2 and 3) from 1 year 3 months of age and 14 days of age to 22 and 20 years of age, respectively. All three patients were followed up at our outpatient department every 3 months for prescription refills. Data on clinical symptoms/signs, electroencephalography (EEG), brain magnetic resonance imaging (MRI), whole-exome sequencing, treatment records including medications, neuromodulation and epilepsy surgery, and clinical outcomes were recorded. Structural prediction and molecular analyses of the novel missense ADGRG1/GPR56 variant (p.Leu290Pro) were performed using computational algorithms and biochemical and cellular techniques, respectively.

2.2 | Brain MRI

MRI was performed at the time of initial diagnosis (1 year of age in Patient 1, and 1 month of age in Patients 2 and 3), follow-up, and post-callosotomy (19 years of age) (Figure S1). MRI was performed using 1.5 T (Magnetom, Siemens), 3 T MRI, with a slice thickness from 3 to 7 mm. The initial brain MR images during infancy were previously reported in 2000,¹⁰ with the impression of genetic-related polymicrogyria.

2.3 | EEG

EEG was obtained using a Natus Nicolet monitor at 1, 5, 9, and 19 years of age in Patient 1; at 3, 9, 10, and 18 years of age in Patient 2; and at 4, 5, 6, 7, 8, 10, and 19 years of age in Patient 3 (Figure S1). The examinations were performed using silver-chloride, gold-plated electrodes placed according to the 10-20 International system, with recorded impedances of less than 5 k Ω at all electrodes. Routine and long-term video monitoring were recorded as bipolar montage and A1A2 reference montage. Initial analog signal conditioning included a 0.0-0.1 Hz high-pass filter, a 30-70 Hz low-pass filter, and a 60 Hz notch filter. The digital sampling rate was 200-500 per second. The patients were sedated with chloral hydrate oral solution during sleep EEG. Sleep and awake EEG were recorded for 30 minutes.

2.4 | Genetic analysis

Whole-exome sequencing (WES)¹¹ followed by Sanger confirmation was performed in Patient 1 at the age of 19 years, and in Patients 2 and 3 at the age of 18 years.

2.5 | Structural prediction and molecular analysis of the novel missense ADGRG1 variant

In silico studies of DynaMut,¹² DynaMut2¹³ and mCSM-membrane¹⁴ were used to predict changes in Gibbs free energy (ΔG) and differences in vibrational entropy (ΔS_{vib}) of several reported BFPP-associated GPR56 mutant proteins compared to those of the GPR56-WT and GPR56-L290P receptors. For the biochemical and molecular characterization of the GPR56-L290P protein, typical flow cytometry and Western blotting analyses were performed, and the results were compared with GPR56-WT and other BFPP-associated point mutants using anti-GPR56 CG2 and CG4 mAbs to verify the potential disease-causing mechanism as described previously.⁷

3 | RESULTS

3.1 | Clinical manifestation

The three siblings are offspring of non-consanguineous parents with one elder sister (Patient 1) and two identical twin younger brothers (Patients 2 and 3) (Figure 1A). There was no family history of major congenital malformations, epilepsy, developmental delay, mental retardation, or any other developmental encephalopathies. All family members of the patients were Taiwanese. The pregnancy and delivery of these patients were uneventful, and they were all born at 36 weeks of gestational age via cesarean section due to breech position and twin pregnancy, respectively. The clinical courses of the three siblings were similar, including a healthy newborn period, and first symptoms of motor and language delay during infancy. Severe mental retardation, diplegic spasticity, paroxysmal nystagmus, and seizures developed during the childhood period. Strabismus was only noted in Patient 1, and ataxia was only noted in Patient 3. All could walk independently at around 1.5 years of age and spoke their first meaningful words by the age of 2. The elder sister had one unique symptom of irritable crying every night from infancy to childhood, which has not been mentioned in previous case reports. This symptom was suspected to be a sleep-related problem, such as NREM parasomnia. Only Patient 3 had progressive hydrocephalus, with an increased head circumference, bulging anterior fontanelle, lethargy, and projectile vomiting at 3 months of age. A ventriculo-peritoneal shunt was subsequently inserted. Head drop developed at 9, 3, and 1 year of age in Patients 1, 2, and 3, respectively.

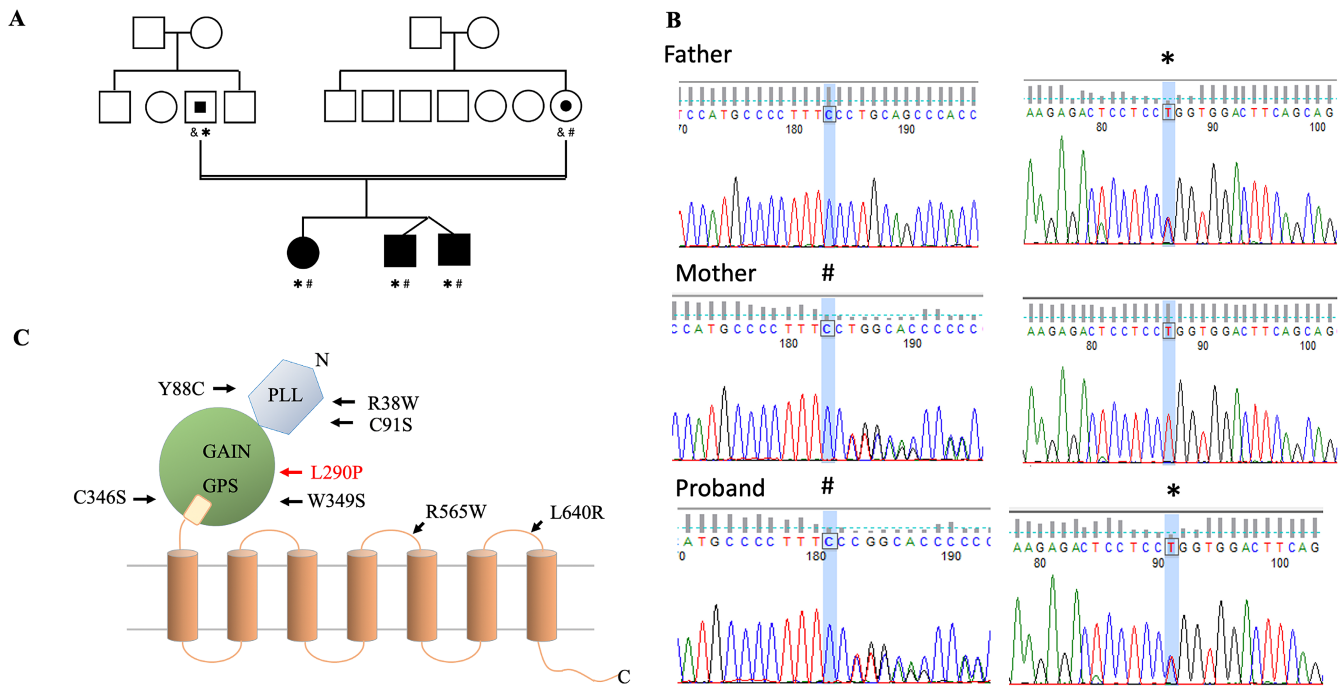


FIGURE 1 Identification of GPR56/ADGRG1 gene frameshift/missense mutations in a Taiwanese family. (A) the family pedigree of the three patients. Squares and circles represent male and female individuals, respectively. White and black represent normal and diseased individuals, respectively. & indicates the GPR56 wild-type sequence, * indicates the L290P missense mutation, while # indicates the frameshift mutation. (B) Results of sanger DNA sequencing of the GPR56/ADGRG1 frameshift (left side) and missense mutations (right side) in diseased patients and their parents. (C) Schematic representation of the GPR56 protein with known BFPP-associated missense point mutations (black arrow) and newly identified L290P mutation (red arrow)

Epilepsy was well controlled with monotherapy of clonazepam, phenobarbital, and valproic acid, respectively, for years. However, refractory epilepsy developed in all three siblings at 11, 12, and 8 years of age, and many types of seizures developed, including tonic, myoclonic, staring, and generalized tonic-clonic. Finally, epileptic falling seizures occurred about a hundred times per day by 18 years of age in all three patients. Several anti-seizure medications, including vigabatrin, clobazam, oxcarbazepine, zonisamide, perampamil, rufinamide, topiramate, lacosamide, levetiracetam, and lamotrigine were tried, but none provided long-term benefits. Vagus nerve stimulation (VNS) was only performed in Patient 3 at 12 years of age, with a maximum setting of 1.5 mA, after which both seizure frequency and cognitive power improved temporarily for approximately 1 year. Palliative anterior two-thirds corpus callosotomy was performed at 20, 18, and 19 years of age, respectively, after which the epileptic falling seizures disappeared totally. However, recurrent epileptic falling seizures gradually occurred at about 1 year post-operatively in Patients 1 and 2. In contrast, Patient 3 remained free from epileptic falling seizures 1.5 years post-operatively (Table S1).

3.2 | Brain imaging analysis

The first brain MRI was obtained at 1 year of age in Patient 1, and at 2 months of age in Patients 2 and 3 (Figure S1). Diffuse thickening of the cortical gray matter with abnormally small, crowded gyri in the bilateral frontoparietal lobes were observed in all patients, compatible with BFPP. Persistent cavum septum pellucidum and cavum vergae only presented in Patient 3. Follow-up brain MRI at 17, 18, and 19 years of age in Patient 1 (Figure 2A-D), 2 (Figure 2E-H), and 3 (Figure 3I-L) showed stationary BFPP and ventriculomegaly (Figure 2A,E,L). Multiple T2 hyperintense nodules in subcortical white matter were also noted in all three patients (Figure 2B,F,J). The nodular lesions were first seen in the brain MRI of Patients 2 and 3 at 2 and 3 years of age. The location and size of these nodular white matter lesions remained unchanged in subsequent MRI scans. There were also multiple T2 hyperintense straight lines following the orientation of penetrating arterioles at the corona radiata (Figure 2D) in Patient 1, and at the basal ganglion (Figure 2L) in Patient 3. Enlarged perivascular space was impressed. A flattened pons and small cerebellar vermis were present in all patients, and were most severe in Patient 2 (Figure 2C,G,K).

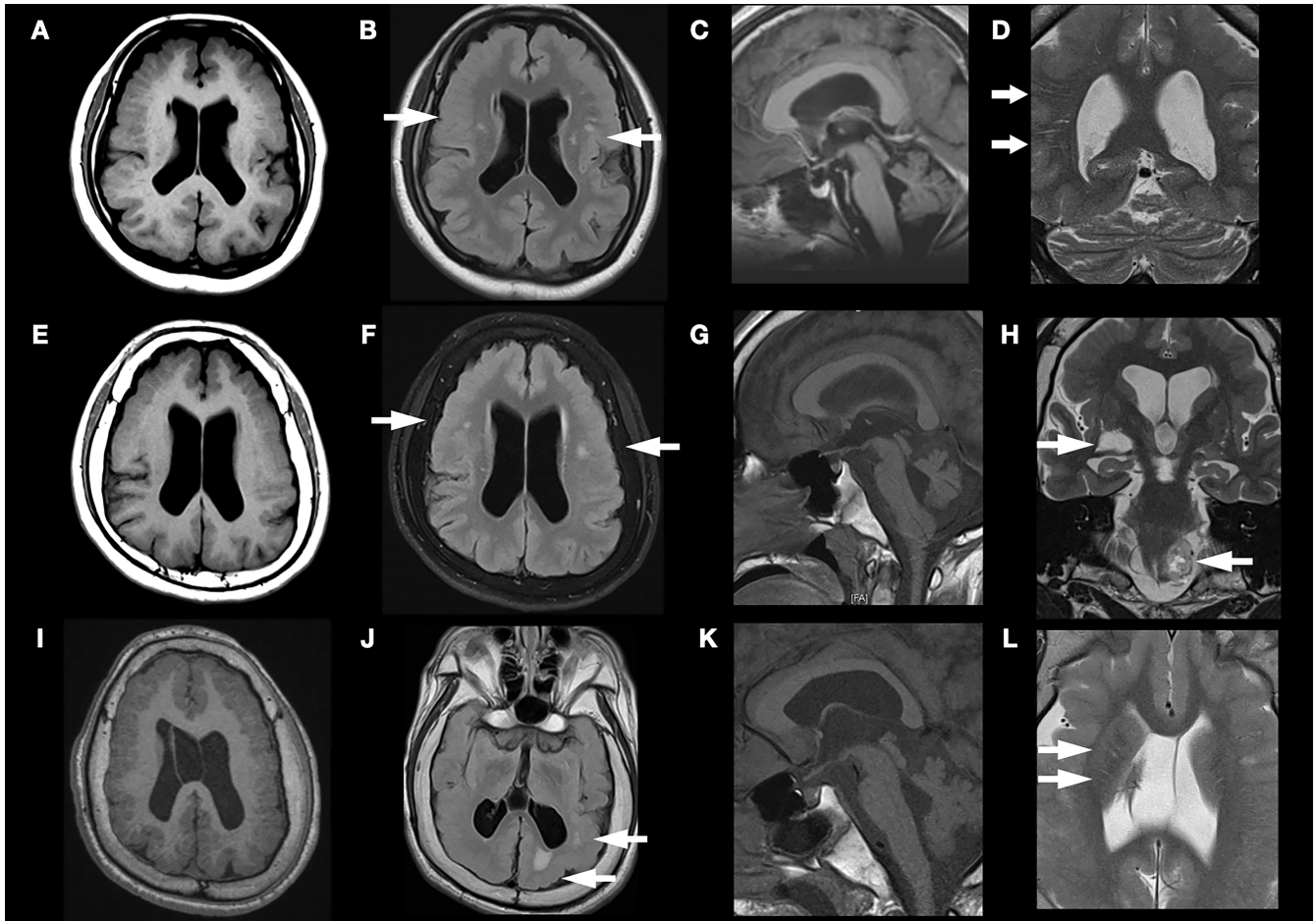


FIGURE 2 Brain magnetic resonance imaging of bilateral frontoparietal polymicrogyria in adults A-D refer to Patient 1; E-H refer to Patient 2; I-L refer to Patient 3. Absence of gyrus, sulcus, and fused, thick cortex distributed over bilateral frontoparietal areas, and ventriculomegaly in images a, e, and i. multiple T2 hyperintense nodules at subcortical white matter shown by the white arrows in images B,F,J. flattened pons and small cerebellar vermis in images C,G,K, cavum septum pellucidum and cavum verger were noted only in Patient 3 in image I. left cerebellar-medullary cistern schwannoma, and right tumefactive perivascular space (1 x 1.4 cm) found at right inferior basal ganglion in Patient 2 in image H. linear enlarged perivascular space over bilateral white matter in image D and over right internal capsular in image L

One tumefactive perivascular space (1 x 1.4 cm) was found at the right inferior basal ganglion (Figure 2H), and a T2 hyperintense mass with central necrosis (2.3 x 1.5 cm) at the left peri-medullary cistern, thought to be a schwannoma, was found in Patient 2 (Figure 2H). A small cystic cavity was also noted in the right frontal periventricular white matter in Patient 1 (Figure 2A,B).

3.3 | EEG analysis

Sleep EEGs were obtained at 1 and 5 years of age in Patient 1; at 3, 9, and 10 years of age in Patient 2; and at 4, 5, 6, and 8 years of age in Patient 3. Awake EEGs were obtained at 9 and 19 years of age in Patient 1; at 18 years of age in Patient 2; and at 7, 10, and 19 years of age in Patient 3. Video EEGs were obtained before callosotomy in Patient 1 and 2 (Table 1).

3.3.1 | High-amplitude rhythmic activity

Intermittent diffuse high-amplitude (>300 uV) rhythmic alpha range (8~12Hz) activity with frontal, central, and temporal predominance (Figure 3A,B) was noted in the sleep EEG at 1 and 5 years of age in Patient 1, and at 4 and 5 years of age in Patient 3 (Table 1). The background was normal at 10~12 Hz and 8~10 uV during these examinations, and there were no interictal epileptic discharges. This activity could have been a sleep spindle, as no normal sleep spindle was seen in the examinations. However, it had a higher amplitude and longer duration (up to 13 seconds) compared to a normal sleep spindle. In Patient 1, this high-amplitude rhythmic activity became continuous in the whole sleep EEG examination at 5 years of age (Figure 3B). In addition, this activity disappeared and was replaced by multifocal sharp waves at 9 and 6 years of age in Patients 1 and 3 (Table 1).

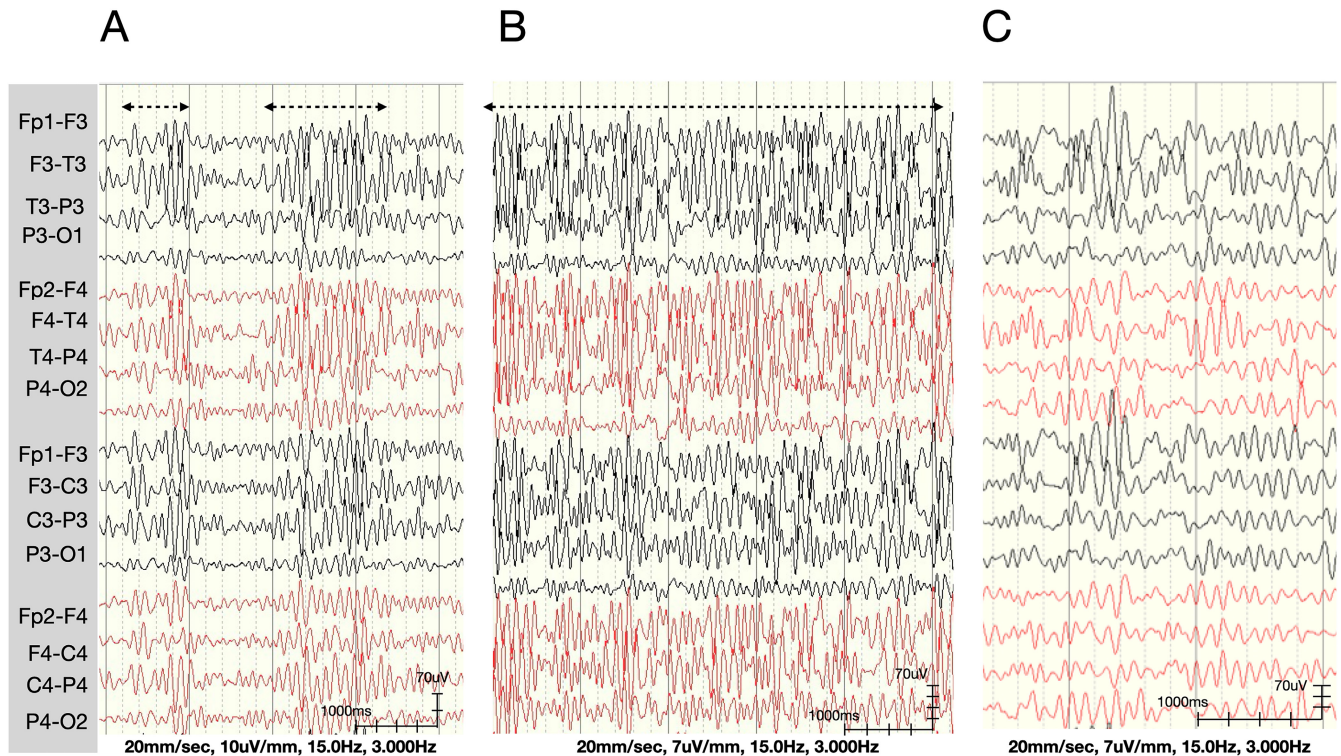


FIGURE 3 Sleep EEG of Patient 1 at 1, 5, and 9 y of age (A-C) with a montage of double banana, speed 30 mm, sensitivity 7(B,C), 10 (a) uV, high cut 15 Hz, low cut 3 Hz. Bilateral extremely high-amplitude (300~400 uV) alpha activity was noted over the frontal, temporal, and parietal lobes (A,B). The duration evolved from 1 to 13 s to continuous at 1 and 5 y of age, respectively (A,B). At 9 y of age, the frequency and amplitude of the alpha activity became lower (C). This activity could have indicated extreme sleep spindles

3.3.2 | Interictal epileptic discharge

Interictal epileptic discharges were first noted at 9, 3, and 6 years of age in Patients 1, 2, and 3, respectively (Table 1). They presented as multifocal sharp waves and resembled brief (1~2 s) alpha activity (Figure 4A). During follow-up, more spiky multifocal interictal epileptic discharges developed in all three patients. Generalized spikes and waves were noted in Patient 2 at 10 and 18 years of age. The background was within theta activity during these periods.

3.3.3 | Post-callosotomy EEG changes

The multifocal sharp waves disappeared, and the theta background changed to a low-amplitude beta rhythm after callosotomy in all patients (Figure 4C). A few bilateral focally independent spikes were still noted in Patient 1, with intermittent generalized spikes and waves, and generalized paroxysmal fast activity, especially during sleep, in Patient 2. No focal spikes, sharp waves, generalized spikes and waves, or generalized paroxysmal fast activity were noted in Patient 3.

3.4 | Genetic analysis

Whole-exome sequencing followed by Sanger confirmation showed that all three patients shared the same compound heterozygous *ADGRG1* alleles (reference transcript: NM_001145773). One allele contained a single-nucleotide deletion at exon 4 leading to a frameshift variant with a premature stop codon which was inherited from the mother (Chr16:57685260C>-, exon 4: c.213delC: p.Pro72Leu fs*40). The other harbored a single-nucleotide missense variant at exon 7 which was inherited from the father (Chr16:57689411, exon 7: c.T869C: p.Leu290Pro) (Figure 1B). Neither allele was found in control population databases (such as ExAc or gnomAD) or a Taiwanese population database (Taiwan Biobank). The frameshift variant was reported to be pathogenic in the ClinVar database, while the missense variant was predicted to be deleterious by multiple in silico algorithms including PolyPhen2, PROVEAN, MutationTaster2, and CADD (data not shown). The L290P missense variant was novel and classified as being likely pathogenic based on the ACMG guidelines under a recessive in trans model, which is consistent with the known inheritance pattern of BFPP-associated *ADGRG1* gene variants (Figure 1B).

TABLE 1 The evolution of electroencephalography (EEG) abnormalities

	Patient 1	Patient 2	Patient 3
EEG Timing (years old)			
Sleep EEG	1, 5	3, 9, 10	4, 5, 6, 8
Awake/Sleep EEG	9, 19	18	7, 10, 19
Video EEG	19	18	
EEG abnormalities			
HARA			
Age (years old)	1, 5	Nil	4, 5
Frequency (Hz)	8-12		8~12
Location	Frontal, Temporal, Parietal		Frontal, Temporal, Parietal
Amplitude (uV)	300-400		150~400
Intermittent Theta/Alpha Epileptiform Activity			
Onset (years old)	9	3	6
Disappearance	Post-callosotomy	Post-callosotomy	Post-callosotomy
Duration (seconds)	1-4 s	0.5~1 s	0.5-2 s
Amplitude (uV)	100-150uV	100~200uV	90-150uV
Location	Diffuse	Bilateral Frontal, Central, Temporal	Diffuse
Typical Epileptic Discharges			
Spike or sharp wave	19	3, 9	6, 8, 10, 11
Onset (years old)			
Location	Bilateral F, C, P	Bilateral F, C	Bilateral F, C, T, O
GSW			
Onset (years old)	Nil	10, 18	Nil
GPFA			
Onset (years old)	Nil	18	Nil

Abbreviations: C, Central; F, Frontal; GPFA, generalized paroxysmal fast activity; GSW, generalized spike and wave; HARA, high-amplitude rhythmic activity; O, Occipital; P, Parietal; T, Temporal.

*Post-Callosotomy.

3.5 | Structural prediction and molecular analysis of the GPR56-L290P variant

Previous studies have shown that almost all BFPP-causing GPR56 mutant receptors are structurally unstable with very weak or no surface expression.⁷ To investigate the possible effect of the L290P mutation on protein stability, we first compared the amino acid sequences of the ECR of the GPR56 receptor from different animal species. Interestingly, multiple sequence alignment showed that all previously reported BFPP-associated mutation residues in the GPR56-ECR, namely R38, Y88, C91, C346, and W349, are highly conserved in all animal species. In contrast, the leucine (L) residue at amino acid 290 of human GPR56 is located within the GAIN domain and conserved in all primates, but is changed to valine (V) in rodents (Figure 5A). Regardless of the change, leucine (L) is still very similar to valine (V) biochemically, but a change in leucine (L) to structurally different proline (P)

is likely to cause significant alterations in intramolecular interactions among residues. To explore the impact of the L290P mutation on protein structural stability, we used DynaMut,¹² DynaMut2,¹³ and mCSM-membrane¹⁴ to predict changes in Gibbs free energy (ΔG) and differences in vibrational entropy (ΔS_{vib}) of several mutant proteins compared to those of the WT receptor to predicted via either the AlphaFold2^{15,16}, RoseTTAFold¹⁷ or TrRosetta.¹⁸ The results showed that the GPR56-L290P isoform, as with the GPR56-C91S and -C346S variants, also displayed a decrease in stability (negative predicted $\Delta\Delta G$) and increase in vibrational entropy (positive $\Delta\Delta S_{\text{vib}}$) (Figure 5B). These features suggested that the GPR56-L290P isoform would be pathogenic with structural instability and increased molecular flexibility.

To verify the disease-causing mechanism of the GPR56-L290P isoform, we next determined the cell surface and total expression levels of the receptor using flow cytometry and Western blotting analyses and compared

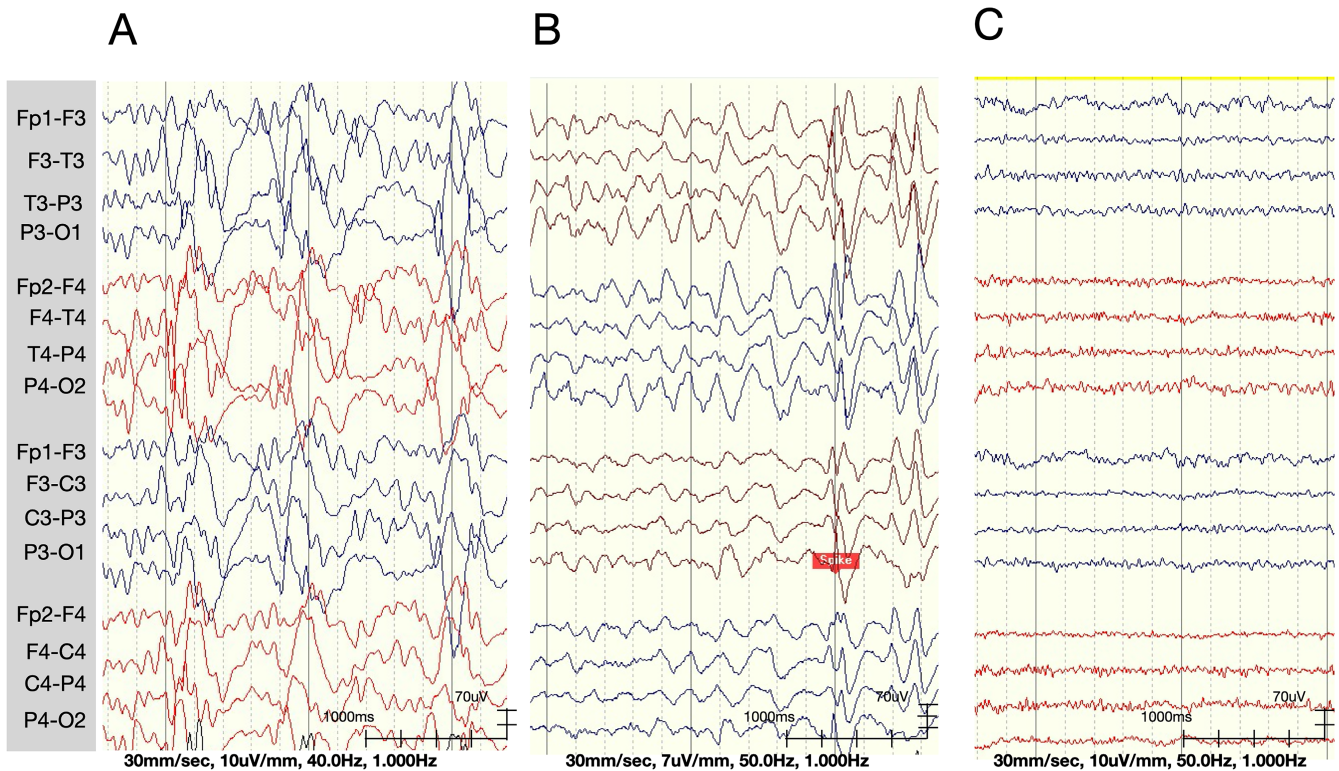


FIGURE 4 Sleep EEG in Patient 2 at 10y of age (A), and awake EEG in Patient 2 at 18 y of age before and after callosotomy (B,C) with a montage of double banana, speed 30 mm, sensitivity 10 (A,C), 7 (B) uV, high cut 40 (A), 50 (B,C) Hz, low cut 3 Hz. Figure a indicates 1 Hz generalized spike and wave during sleep, Figure B shows diffuse theta activity at 18 y of age with intermittent generalized spike and wave. Figure C shows that the abnormal theta activity almost completely disappeared after callosotomy, which might indicate that the theta activities were related to interictal epileptic discharges rather than cortical dysfunction

the results with GPR56-WT and other BFPP-associated point mutants. Highly similar to those of the GPR56-C91S, -C346S, and -R565W isoforms, a markedly reduced surface level of GPR56-L290P was detected in transiently transfected HEK-293T cells (Figure 5C). In contrast, the total cellular expression of GPR56-L290P was comparable with those of GPR56-WT and BFPP-associated mutants (Figure 5C). These results indicated that the L290P mutation caused a reduction in cell surface GPR56 expression as a result of impaired subcellular trafficking, likely due to receptor instability. This conclusion was confirmed using Western blotting analysis, which showed much weaker protein signals in the lysates of cells expressing GPR56-L290P than in those expressing the WT receptor (Figure 5D). Furthermore, the Western blotting results revealed that the L290P isoform, as with the C346S isoform, was not processed by GPS proteolysis, as protein bands of the same size were detected by two different Abs used to detect the extracellular fragment and transmembrane fragment, respectively (Figure 5D). Thus, we concluded that the GPR56-L290P variant is a GPS proteolysis-deficient unstable receptor which is retained mostly in the intracellular compartment.

4 | DISCUSSION

The three members of the same family reported in this study are the first genetically confirmed BFPP cases in Taiwan, in whom we detected one frameshift mutation and one novel missense variant (Leu290Pro) of ADGRG1/GPR56 (Figure 1). There are two novel findings in this study, the epileptogenic course in BFPP and EEG abnormalities after callosotomy, and the pathogenic mechanism of the Leu290Pro variant.

Polymicrogyria is associated with high epileptogenicity, and more extensive distribution of polymicrogyria is associated with early seizure onset.¹⁹ All three patients underwent a similar epileptogenesis course, including pre-epilepsy, pharmacoresponse, and pharmacoresistant periods. The onset of seizures began after developmental delay, and ranged from 1 to 9 years of age. No focal epileptic discharges were noted before seizure onset, however bilateral high-amplitude rhythmic activity over frontal, parietal, and temporal regions developed during sleep. This could have been an extreme sleep spindle, which has been reported in patients with lissencephaly syndrome,²⁰ but this is the first reported case in patients with

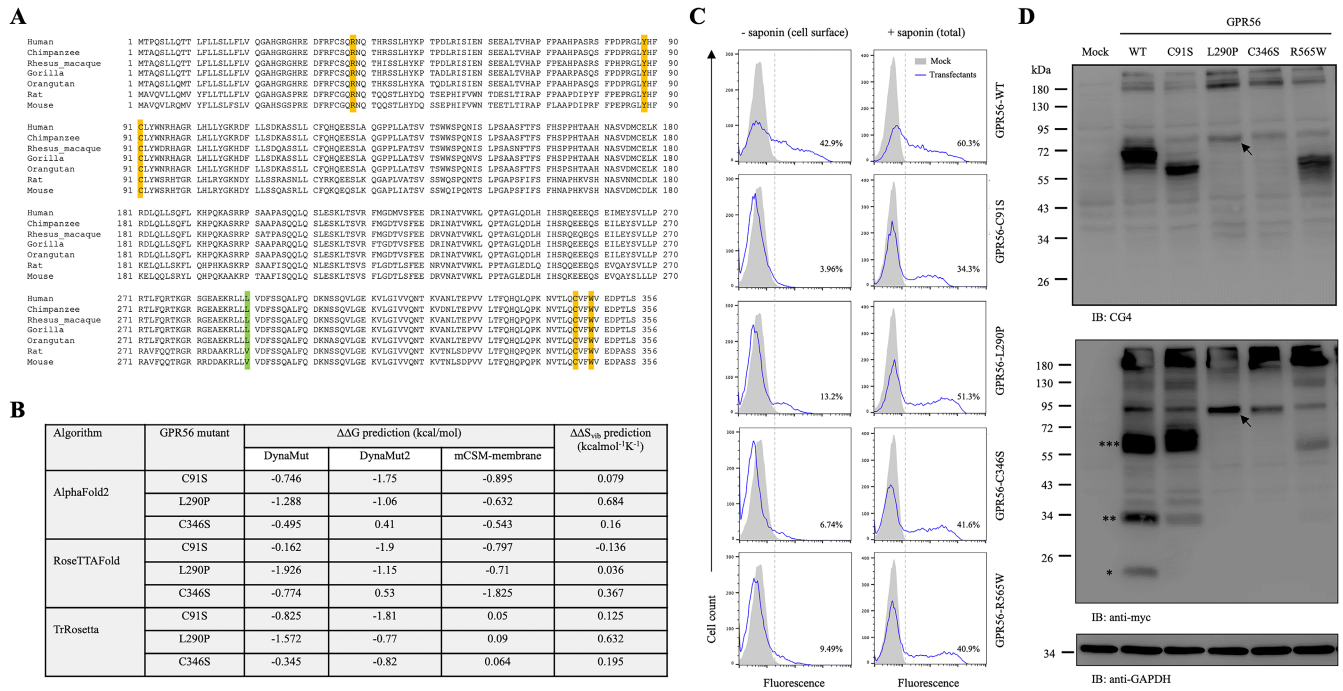


FIGURE 5 (A) Alignment and comparison of the amino acid sequences of ADGRG1/GPR56-ECR from the following animal species: Human (*Homo sapiens*), Chimpanzee (*Pan troglodytes*), Rhesus macaque (*Macaca mulatta*), Western lowland gorilla (*Gorilla gorilla gorilla*), Bornean orangutan (*Pongo pygmaeus*), Rat (*Rattus norvegicus*), and Mouse (*Mus musculus*). The known BFPP-associated mutant residues (R38, Y88, C91, C346, and W349) are highlighted in yellow. The newly identified L290 residue is highlighted in green. (B) Table summarizing the predicted $\Delta\Delta G$ by DynaMut, DynaMut2, and mCSM-membrane; and $\Delta\Delta S_{vib}$ for the GPR56-C91S, -L290P, and -C346S mutants using the AlphaFold2-, RoseTTAFold-, or TrRosetta-predicted structures compared to the WT structure. Negative $\Delta\Delta G$ denotes protein destabilization, while a positive value denotes protein stabilization. Positive $\Delta\Delta S_{vib}$ denotes an increase in molecular flexibility, while a negative value denotes a decrease in molecular flexibility. (C) Flow cytometry analysis of cell surface (without saponin) and total cellular expression (with saponin) of the GPR56 receptors expressed in HEK293T transfectant cells as indicated using anti-GPR56 CG2 ab. The gray area represents the mocktransfected control. The numbers shown indicate the percentage of receptor-positive transfectant cells. (D) Western blot analysis of total cell lysates from HEK293T transfectant cells expressing GPR56-WT and relevant BFPP-associated mutants as indicated. Blots were probed with anti-GPR56 CG4 (upper panel) and anti-myc (lower panel) abs to detect the ECR and 7TM subunits, respectively. The monomeric, dimeric, or trimeric forms of the 7TM subunit are indicated by 1, 2, and 3 asterisks, respectively. The arrow denotes the uncleaved single-chain L290P mutant

GPR56-related polymicrogyria. According to Gibbs and Gibbs in 1973,²¹ an extreme spindle is abnormal and correlated with the organic type of mental retardation. These spindles can be classified into six types, of which type 3 involves more spikes and is associated with the highest incidence of epilepsy. Sleep spindles are generated from the thalamic reticular nucleus, regulated in thalamocortical loops, and are associated with memory consolidation and cognitive abilities.²² An extreme spindle may indicate cortical excitation and inhibition imbalance, as in our cases.

Head drop was the first type of seizure in our patients, followed by several other kinds of seizures including tonic, generalized tonic clonic, myoclonic, staring, and epileptic falling. Various types of seizures have been reported in patients with BFPP, including generalized tonic clonic,^{5,23,24} atypical absence,^{5,23} epileptic spasm,^{5,25} tonic,^{25,26} atonic,²³ and recurrent nonconvulsive status epilepticus.⁵ Our three cases presented with multiple types of seizures, epileptic

falling, mental retardation, slow background, and multiple focal spikes in EEG. However, slow generalized spikes and waves (1.5 Hz) and generalized paroxysmal fast activity were only noted in Patient 2 (Table 1).

Other than typical brain imaging findings of BFPP in our patients, the straight linear T2 hyperintense white matter lesions vertical to the cortex in Patients 1 and 3 were distinct, and may reflect an enlarged perivascular space. These lesions have not been discussed in patients with BFPP before, however, they have been reported in patients with polymicrogyria.²⁷ These lesions may be due to focal white matter atrophy.

Traditional anterior 2/3 corpus callosotomy has been shown to have an excellent effect on seizure control, especially epileptic drop attacks.²⁸ However, there was a honeymoon effect with regard to seizure control after surgery in our cases. To achieve a more persistent therapeutic effect, more extensive disconnection should be considered,

including total corpus callosotomy and/or transection of the anterior and posterior commissure, although both surgeries are associated with increased risks of paraoperative and postoperative complications. Of note, Patient 3 received concurrent VNS treatment, and his epilepsy remained well controlled with no epileptic falling seizures noted 1.5 years later. In palliative surgery, corpus callosotomy is thought to potentially be more effective than VNS in reducing seizure frequency.²⁹ On the other hand, Katagiri et al. reported that combining callosotomy and VNS resulted in satisfactory treatment outcomes in patients with Lennox–Gastaut syndrome,³⁰ while Hong et al. also supported that callosotomy can help reduce seizures in patients with medically refractory epilepsy following VNS.³¹ The better outcome in Patient 3 suggests that these two surgical interventions are complementary and can work synergistically in particularly refractory patients. In other words, surgery would be more beneficial when combined with VNS than either one alone.

According to the ClinVar database, there are 32 *ADGRG1* pathogenic and likely pathogenic mutations, of which 21 are protein-truncating variants and 11 are missense variants located in both the extracellular and transmembrane domains. In our cases, the novel frameshift variant (p.Pro72Leufs*40) was located at the pentraxin/laminin/neurexin/sex-hormone-binding-globulin-like (PLL) domain of GPR56-ECR, while the missense variant (p.Leu290Pro) was within the GAIN domain. As the frameshift mutation was predicted to produce a non-functional truncated GPR56 protein, we focused on the molecular analysis of the GPR56-L290P isoform. Structural prediction based on multiple computational algorithms suggested that this variant was pathogenic and likely an unstable receptor molecule (Figure 5B). Indeed, our expression and biochemical analyses confirmed that the GPR56-L290P isoform was weakly expressed on the cell surface due to structural instability and impaired intracellular trafficking (Figure 5C). In addition, it was not modified properly by GPS auto-proteolysis (Figure 5D). This is probably because the L290P mutation is located within the GAIN domain, which is known to be essential for the GPS proteolytic modification of most aGPCRs. This conclusion was supported by the fact that the GPR56-L290P isoform shared very similar expression and biochemical characteristics with the GPR56-C346S isoform, in which the mutated residue was located within the GPS motif that disrupted the GPS auto-proteolysis (Figure 1C).

Our data were obtained from three cases of one family, and the timing of data collection was inconsistent during long-term follow-up. This limits the strength of the findings. However, the findings of EEG changes from childhood to adulthood, and post-callosotomy in our cases with

BFFF may lead to further well-designed studies to elucidate the relationship between polymicrogyria and brain function development.

In conclusion, we found sleep EEG findings of high-amplitude rhythmic activity in our cases with BFPP only during infancy and childhood, and confirmed that the missense variant (p.Leu290Pro) led to loss of function due to impaired receptor auto-proteolysis, intracellular trafficking, and surface expression.

AUTHOR CONTRIBUTIONS

The electroclinical data were analyzed by Cheng-Yen Kuo, MD, Kuang-Lin Lin, MD, Jainn-Jim Lin, MD, and Po-Cheng Hung, MD. The genetic analysis was performed by Meng-Han Tsai, MD, PhD, and the Kaohsiung Epilepsy and Neurogenetics Research Program of Chang Gung Memorial Hospital, and the Genomic & Proteomic Core Laboratory at the Department of Medical Research, Kaohsiung Chang Gung Memorial Hospital. The biological analysis of GPR56-L290P variant structural and function analysis was performed by Hsi-Hsien Lin, PhD and Abhishek Kumar Singh of the Department of Microbiology and Immunology, College of Medicine, Chang Gung University, Taoyuan, Taiwan. Surgery was performed Yu-Chi Wang MD, PhD. The brain image analysis was performed by Chang-Chih Chen, MD.

ACKNOWLEDGMENTS

The authors thank Min-Lan Tsai MD for support with the electroclinical analysis.

FUNDING INFORMATION

This study was supported in part by a grant from Chang Gung Memorial Hospital (CMRPG3H0761–3).

CONFLICT OF INTEREST

None of the authors have any conflicts of interest to disclose. We confirm that we have read the Journal's position on issues involved in ethical publication and affirm that this report is consistent with those guidelines.

ETHICAL APPROVAL

This study was approved by the Chang Gung Memorial Hospital Institutional Review Board (202101571B0).

ORCID

Cheng-Yen Kuo  <https://orcid.org/0000-0002-8406-3660>
 Meng-Han Tsai  <https://orcid.org/0000-0002-4570-5712>

REFERENCES

- Leventer RJ, Jansen A, Pilz DT, Stoodley N, Marini C, Dubeau F, et al. Clinical and imaging heterogeneity of polymicrogyria: a study of 328 patients. *Brain*. 2010;133(Pt 5):1415–27.

2. Piao X, Hill RS, Bodell A, Chang BS, Basel-Vanagaite L, Straussberg R, et al. G protein-coupled receptor-dependent development of human frontal cortex. *Science*. 2004;303(5666):2033–6.
3. Singh AK, Lin HH. The role of GPR56/ADGRG1 in health and disease. *Biom J*. 2021;44(5):534–47.
4. Hamann J, Aust G, Arac D, Engel FB, Formstone C, Fredriksson R, et al. International union of basic and clinical pharmacology. XCIV. adhesion G protein-coupled receptors. *Pharmacol Rev*. 2015;67(2):338–67.
5. Parrini E, Ferrari AR, Dorn T, Walsh CA, Guerrini R. Bilateral frontoparietal polymicrogyria, Lennox-Gastaut syndrome, and GPR56 gene mutations. *Epilepsia*. 2009;50(6):1344–53.
6. Jin Z, Tietjen I, Bu L, Liu-Yesucevitz L, Gaur SK, Walsh CA, et al. Disease-associated mutations affect GPR56 protein trafficking and cell surface expression. *Hum Mol Genet*. 2007;16(16):1972–85.
7. Chiang NY, Hsiao CC, Huang YS, Chen HY, Hsieh IJ, Chang GW, et al. Disease-associated GPR56 mutations cause bilateral frontoparietal polymicrogyria via multiple mechanisms. *J Biol Chem*. 2011;286(16):14215–25.
8. Bahi-Buisson N, Poirier K, Boddaert N, Fallet-Bianco C, Specchio N, Bertini E, et al. GPR56-related bilateral frontoparietal polymicrogyria: further evidence for an overlap with the cobblestone complex. *Brain*. 2010;133(11):3194–209.
9. Chang BS, Piao X, Bodell A, Basel-Vanagaite L, Straussberg R, Dobyns WB, et al. Bilateral frontoparietal polymicrogyria: clinical and radiological features in 10 families with linkage to chromosome 16. *Ann Neurol*. 2003;53(5):596–606.
10. Hung PC, Wang HS. Polymicrogyria in monozygous twins and an elder sibling. *Dev Med Child Neurol*. 2003;45(7):494–6.
11. Tsai MH, Chan CK, Chang YC, Yu YT, Chuang ST, Fan WL, et al. DEPDC5 mutations in familial and sporadic focal epilepsy. *Clin Genet*. 2017;92(4):397–404.
12. Rodrigues CH, Pires DE, Ascher DB. DynaMut: predicting the impact of mutations on protein conformation, flexibility and stability. *Nucleic Acids Res*. 2018;46(W1):W350–W5.
13. Rodrigues CHM, Pires DEV, Ascher DB. DynaMut2: assessing changes in stability and flexibility upon single and multiple point missense mutations. *Protein Sci*. 2021;30(1):60–9.
14. Pires DEV, Rodrigues CHM, Ascher DB. mCSM-membrane: predicting the effects of mutations on transmembrane proteins. *Nucleic Acids Res*. 2020;48(W1):W147–W53.
15. Mirdita M, Schutze K, Moriwaki Y, Heo L, Ovchinnikov S, Steinegger M. ColabFold: making protein folding accessible to all. *Nat Methods*. 2022;19(6):679–82.
16. Jumper J, Evans R, Pritzel A, Green T, Figurnov M, Ronneberger O, et al. Highly accurate protein structure prediction with AlphaFold. *Nature*. 2021;596(7873):583–9.
17. Baek M, DiMaio F, Anishchenko I, Dauparas J, Ovchinnikov S, Lee GR, et al. Accurate prediction of protein structures and interactions using a three-track neural network. *Science*. 2021;373(6557):871–6.
18. Yang J, Anishchenko I, Park H, Peng Z, Ovchinnikov S, Baker D. Improved protein structure prediction using predicted interresidue orientations. *Proc Natl Acad Sci U S A*. 2020;117(3):1496–503.
19. Shain C, Ramgopal S, Fallil Z, Parulkar I, Alongi R, Knowlton R, et al. Polymicrogyria-associated epilepsy: a multicenter phenotypic study from the epilepsy phenome/genome project. *Epilepsia*. 2013;54(8):1368–75.
20. Hakamada S, Watanabe K, Hara K, Miyazaki S. The evolution of electroencephalographic features in lissencephaly syndrome. *Brain Dev*. 1979;1(4):277–83.
21. Gibbs EL, Gibbs FA. Clinical correlates of various types of extreme spindles. *Clin Electroencephalogr*. 1973;4(2):89–100.
22. Fernandez LMJ, Luthi A. Sleep spindles: mechanisms and functions. *Physiol Rev*. 2020;100(2):805–68.
23. Piao X, Basel-Vanagaite L, Straussberg R, Grant PE, Pugh EW, Doheny K, et al. An autosomal recessive form of bilateral frontoparietal polymicrogyria maps to chromosome 16q12.2-21. *Am J Hum Genet*. 2002;70(4):1028–33.
24. Luo R, Yang HM, Jin Z, Halley DJ, Chang BS, MacPherson L, et al. A novel GPR56 mutation causes bilateral frontoparietal polymicrogyria. *Pediatr Neurol*. 2011;45(1):49–53.
25. Fujii Y, Ishikawa N, Kobayashi Y, Kobayashi M, Kato M. Compound heterozygosity in GPR56 with bilateral frontoparietal polymicrogyria. *Brain Dev*. 2014;36(6):528–31.
26. Sawal HA, Harripaul R, Mikhailov A, Vleuten K, Naeem F, Nasr T, et al. Three mutations in the bilateral Frontoparietal Polymicrogyria gene GPR56 in Pakistani intellectual disability families. *J Pediatr Genet*. 2018;7(2):60–6.
27. Hayashi N, Tsutsumi Y, Barkovich AJ. Polymicrogyria without porencephaly/schizencephaly. MRI analysis of the spectrum and the prevalence of macroscopic findings in the clinical population. *Neuroradiology*. 2002;44(8):647–55.
28. Bower RS, Wirrell E, Nwojo M, Wetjen NM, Marsh WR, Meyer FB. Seizure outcomes after corpus callosotomy for drop attacks. *Neurosurgery*. 2013;73(6):993–1000.
29. Rolston JD, Englot DJ, Wang DD, Garcia PA, Chang EF. Corpus callosotomy versus vagus nerve stimulation for atonic seizures and drop attacks: a systematic review. *Epilepsy Behav*. 2015;51:13–7.
30. Katagiri M, Iida K, Kagawa K, Hashizume A, Ishikawa N, Hanaya R, et al. Combined surgical intervention with vagus nerve stimulation following corpus callosotomy in patients with Lennox-Gastaut syndrome. *Acta Neurochir*. 2016;158(5):1005–12.
31. Hong J, Desai A, Thadani VM, Roberts DW. Efficacy and safety of corpus callosotomy after vagal nerve stimulation in patients with drug-resistant epilepsy. *J Neurosurg*. 2018;128(1):277–86.

SUPPORTING INFORMATION

Additional supporting information can be found online in the Supporting Information section at the end of this article.

How to cite this article: Kuo C-Y, Tsai M-H, Lin H-H, Wang Y-C, Singh AK, Chen C-C, et al. Identification and clinical characteristics of a novel missense ADGRG1 variant in bilateral Frontoparietal Polymicrogyria: The electroclinical change from infancy to adulthood after Callosotomy in three siblings. *Epilepsia Open*. 2023;00:1–11. <https://doi.org/10.1002/epi4.12685>